Published in final edited form as:
Angew Chem Int Ed Engl. 2010 June 1; 49(24): 4088–4091. doi:10.1002/anie.201001199.

Access to Well-Defined Ru(I) and Os(I) Metalloradicals**

Ayumi Takaoka[ζ], **Laura C. H. Gerber**, and **Jonas C. Peters**[ζ]
Department of Chemistry, Massachusetts Institute of Technology, Cambridge, MA 02139 (USA)

Abstract

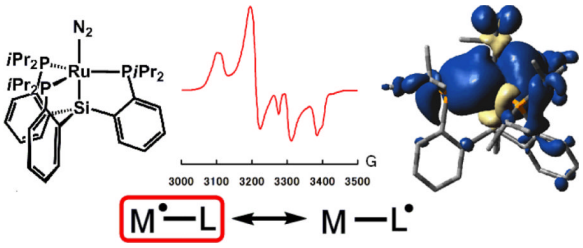

The first examples of well-defined mononuclear Ru(I) and Os(I) complexes have been prepared and crystallographically characterized. EPR spectroscopy and DFT calculations indicate metalloradical character. The Ru(I) and Os(I) metalloradicals exhibits both 1-electron and 2-electron redox reactivity. The latter process affords unusual imido/nitrene complexes with substantial radical character on the “ArN” moiety.

Keywords

Ruthenium; Osmium; Nitrogen; Radicals; Group Transfer

Low-valent metalloradicals of the late second and third row transition metals have garnered recent attention in the context of their interesting spectroscopic properties and potential applicability in catalysis.[1] Mononuclear Ru(I) and Os(I) compounds of such types are particularly sparse.[2] Due to the inherent instability of these species, studies that extend beyond attempts to rapidly characterize them *in situ* are not available. As a consequence the chemistry of mononuclear Ru(I) and Os(I) complexes is essentially unexplored.[3]

Recently we reported the first mononuclear complexes of Fe(I) with terminal dinitrogen ligands.[4] The iron centers in these complexes are chelated by bulky tetradentate tris(phosphino)silyl ligands, $[SiP^{R}_{3}]^{-}$ ($[SiP^{R}_{3}]^{-}$ = $(2\text{-}R_2PC_6H_4)_3Si^{-}$, R = Ph, *i*Pr), that favor monorather than dinuclear species. The steric influence provided by this scaffold and its ability to accommodate the Fe(I) oxidation state made it a plausible candidate for exploring access to the unusual oxidation states Ru(I) and Os(I). Herein we report structural, spectroscopic, and theoretical studies of well-defined and mononuclear Ru(I) and Os(I) complexes, $[SiP^{iPr}_{3}]M(L)$ (M = Ru, Os; L = N_2, PMe_3). To our knowledge, these are the first such examples to be isolated and thoroughly characterized, including characterization by X-ray diffraction. Moreover, initial reactivity studies with $[SiP^{iPr}_{3}]M(N_2)$ (M = Ru, Os) complexes expose both one and two-electron reactivity. The latter type affords unusual

**This work was supported by the NIH (GM070757). Samantha MacMillan and Dr. Peter Müller are acknowledged for crystallographic assistance. The NSF is acknowledged for use of instruments at the MIT DCIF (CHE-9808061, DBI-97299592)

ζCurrent address: Division of Chemistry and Chemical Engineering, California Institute of Technology, Pasadena, CA 91125 Fax: (+1)-(626) 395-6948 jpeters@caltech.edu

M(III) imido (M = Ru, Os) complexes, [SiP$^{i\mathrm{Pr}}_3$]M(NAr) (M =Ru, Os; Ar = $C_6H_4CF_3$), that display substantial 'imidyl' radical character. In contrast to its highly unstable and structurally related Fe(III) imido derivative, which can only be observed in a frozen glass,[5] these imidyl radicals are sufficiently long-lived to isolate in pure form.

Precursors to the M(I) (M = Ru, Os) complexes, [SiP$^{i\mathrm{Pr}}_3$]MCl (M = Ru (**1**), Os (**2**)), are prepared by heating a mixture of HSiP$^{i\mathrm{Pr}}_3$, [(η^6-C_6H_6)M(Cl)(μ-Cl)]$_2$, and Et_3N in toluene to yield red **1** and brown **2** in 94% and 95% yield, respectively (Scheme 1). Chemical reduction of **1** and **2** with KC_8 results in green [SiP$^{i\mathrm{Pr}}_3$]M(N_2) (M = Ru (**3**), Os(**4**)) in 85% and 70% yield. The ^{1}H NMR spectra of **3** and **4** are similar and show broad features between δ = -1~11 ppm, consistent with their expected paramagnetism (S = 1/2). The IR spectra of **3** and **4** depict strong vibrations at 2088 and 2052 cm^{-1} for the nitrogen ligands.

Crystals of **3** and **4** suitable for X-ray diffraction are grown from slow evaporation of a concentrated pentane solution. Unlike [SiP$^{i\mathrm{Pr}}_3$]Fe(N_2), which is rigorously trigonal bipyramidal (TBP),[5] the solid-state structures of **3** (Figure 2) and **4** (see SI) feature substantive distortions from TBP geometries (τ= 0.76 (**3**), 0.70(**4**))[6] with one of the P-M-P angles notably larger than the others. The N-N bond lengths are short (1.097(5) (**3**), 1.101(6) (**4**) Å) and consistent with the high ν_{N2} values. The N_2 ligands in **3** and **4** are labile, and addition of one equivalent of PMe_3 results in formation of the phosphine adducts, [SiP$^{i\mathrm{Pr}}_3$]M(PMe_3) (M = Ru (**5**), Os(**6**)). Compound **5** has been crystallographically characterized (see SI) and has a geometry similar to **3** (τ = 0.86).

The cyclic voltammogram of **3** shows one oxidation event at -1.24 V (vs Fc/Fc$^+$), and one reduction event at -2.14 V, which are assigned to the formal Ru$^{II/I}$ and Ru$^{I/0}$ couples, respectively. Chemical oxidation and reduction of **3** with FcBAr$^F_4$ (BAr$^F_4$ = tetrakis(3,5-bis(trifluoromethyl)phenyl)borate) and KC_8 leads to the corresponding Ru(II) and Ru(0) dinitrogen complexes, {[SiP$^{i\mathrm{Pr}}_3$]Ru(N_2)}$^+$BAr$^F_4$$^-$ (**7**) and {[SiP$^{i\mathrm{Pr}}_3$]Ru(N_2)}$^-$K(THF)$_x^+$ (**8**), respectively, which have also been crystallographically characterized (see SI). Complexes **3, 7**, and **8** represent a rare series of mononuclear N_2 complexes spanning three distinct states of oxidation (Scheme 2); the related iron system also stabilizes a corresponding N_2 series.[7] The N_2 ligand in **7** is very labile and appears to be in equilibrium with an N_2 free species,[8] as evidenced by the shift in the Ru$^{II/I}$ couple under argon and its ^{15}N NMR spectrum, which only shows resonances for the coordinated N_2 at low temperature.[9] While the cyclic voltammogram of **4** also displays a reduction event at -1.94 V, an irreversible oxidation event at -1.17 V is observed. The reduction product, {[SiP$^{i\mathrm{Pr}}_3$]Os(N_2)}$^-$K(THF)$_x^+$ (**9**) was accessed similarly to **8** and its solid-state structure is isostructural (see SI).

Although **3-6** are formally Ru(I) and Os(I) complexes, the possibility of a ligand-centered radical cannot be excluded based on structural studies alone, especially in light of the growing recognition of redox non-innocence of many auxiliary ligands.[10] To investigate the distribution of spin density in **3-6**, their EPR spectra were measured at 77 K in toluene glass (Figure 1 and SI). Each spectrum exhibits rhombic features with large hyperfine coupling to one phosphorus atom, consistent with unpaired spin density localized in an orbital of the equatorial plane of the TBP.

In assessing metal radical character, the anisotropy of g-values ($\Delta g = g_{max} - g_{min}$) is particularly noteworthy, since large Δg has been noted as a crude indication of metalloradical character for S = 1/2 systems.[11,12] Overall the Δg values for **3-6**, which are 0.135, 0.257, 0.166, and 0.318 respectively, are significantly larger than complexes that have been assigned as ligand centered radicals.[13,14] The noticeably larger Δg values for the Os relative to the Ru complexes are likely due to a greater spin-orbit coupling constant for the heavier metal.[15] Although g-values alone cannot be used as a quantitative measure

of spin density, the simulated EPR parameters support our formulations of **3-6** as *bona fide* metalloradicals. As a test of our assignment, Mülliken spin densities (SD) were calculated for **3-6** (Figure 2 and SI). These calculations place 76% (**3**), 69% (**4**), 84% (**5**), and 79% (**6**) of the SD at the metal center. In addition 16% (**3**), 15% (**4**), 13% (**5**), and 13% (**6**) of the SD is located at the phosphines.[16] In each complex, one of the P atoms possesses a greater value relative to the other two, consistent with the EPR simulations that suggest an unpaired spin in the equatorial plane.

Chemical evidence consistent with the metalloradical character of **3** is obtained by its treatment with $^{n}Bu_3SnH$, which cleanly affords the hydride complex $[SiP^{iPr}_3]Ru(H)(N_2)$, (**10**), over 24 h; this is similar to the reactivity of other metal-centered radicals towards $^{n}Bu_3SnH$.[17a] In addition, **3** reacts cleanly with I_2 and PhS-SPh to afford the corresponding Ru(II) iodide and thiolate complexes, $[SiP^{iPr}_3]RuI$ and $[SiP^{iPr}_3]RuSPh$ (see SI).

The reactivity of late second and third row metalloradicals often follows one-electron processes.[1,17] Having observed one-electron reactivity in **3** we sought, in turn, to investigate whether two-electron processes might also be feasible. To this end, complex **3** was treated with organoazides to see if metal imido/nitrene species would be formed through loss of N_2, akin to the recently observed reactivity of related Fe(I) complexes.[18] Treatment of **3** with *para*-CF_3 substituted phenylazide led to formation of the formally Ru(III) imido species, $[SiP^{iPr}_3]Ru(NAr)$ Ar = $C_6H_4CF_3$ (**11**). The solid-state structure of **11** (Figure 2) reveals a geometry midway between a TBP (τ = 0.54) and SQP with a Ru-N bond length of 1.869(2) Å. While this bond length is significantly shorter than Ru-N bonds between typical ruthenium anilides (Ru-N > 1.95 Å),[19] it is appreciably longer than prototypical ruthenium imido complexes (Ru-N < 1.80 Å).[20] Treatment of **4** with *para*-CF_3 substituted phenylazide also leads to the corresponding Os(III) imido species $[SiP^{iPr}_3]Os(NAr)$ Ar = $C_6H_4CF_3$ (**12**). Crystallographic characterization establishes that **12** is isostructural to its ruthenium analogue **11** (see SI).

Complexes **11** and **12** represent interesting examples of 5-coordinate, formally d^5 imido complexes. Qualitative molecular orbital diagrams predict low bond orders (less than or equal to 1.5) due to the occupation of π^* orbitals.[21] It is worth underscoring that TBP complexes with metal-ligand multiple bonds and d-electron configurations >1 are virtually unknown. Que and coworkers have provided a noteworthy recent exception.[22] The stability of **11** and **12** is, therefore, surprising and distinct from its chemically related and highly unstable iron derivative $[SiP^{iPr}_3]Fe(N\text{-}p\text{-tolyl})$, which has a calculated geometry[23] close to **11** and **12**. $[SiP^{iPr}_3]Fe(N\text{-}p\text{tolyl})$ is only observable by EPR when generated photolytically in a frozen glass, decomposing rapidly *via* presumed bimolecular nitrene coupling to yield azobenzenes.[5] While complexes **11** and **12** decompose in solution at room temperature over several days, they are stable at -35 °C as solids for extended periods.

The difference in stability/reactivity between $[SiP^{iPr}_3]Fe(NAr)$ and complexes **11** and **12** could potentially be attributed to differences in electronic configuration. Though they are formally M(III) imido complexes, close examination of their EPR spectra indicate that they possess significant nitrogen centered radical character. Unlike the RT spectra of **3-6**, which show broad features, the spectra of **11** and **12** (Figure 1 and SI) show relatively sharp four line patterns with isotropic g-values of 2.02 and 2.01, respectively, which are much closer in value to that of a free electron (g_e = 2.0023) compared to the corresponding metalloradicals **3-6**. Ruthenium and osmium hyperfine coupling are also observed (A^{Ru} = 48 MHz (**11**), A^{Os} = 150 MHz (**12**)) and the spectra are best simulated by assigning hyperfine coupling to one nitrogen atom (A^N = 98 MHz (**11**), A^N = 93 MHz (**12**)) and smaller coupling to one phosphorus atom (A^P = 64 MHz (**11**), A^P = 58 MHz (**12**)). These isotropic A^N values are

surprisingly large. For comparison, the similarly sp-hybridized NO radical has a nitrogen hyperfine coupling constant of A^N = 77 MHz.[24] In addition, the Ru hyperfine coupling constant, A^{Ru}, in **11** is smaller than a spectroscopically detected Ru(III) imido complex that was suggested to possess considerable ligand radical character.[25] Further supporting the largely ligand-centered radical character of **11** and **12**, the EPR spectra at 77 K reveal much smaller g-anisotropies (Δg = 0.072 (**11**), 0.128 (**12**)) relative to their corresponding Ru(I) and Os(I) metalloradicals, **3**-**6**. DFT calculations are consistent with the EPR parameters and show that 54% (**11**) and 54 % (**12**) of the SD is distributed throughout the NAr moiety, of which 27% (**11**) and 24% (**12**) is on the nitrogen atom and 40% (**11**) and 39% (**12**) is located at the metal center (see SI). While delocalization of the spin density along the M-NAr moiety is evident, both EPR and DFT data suggest that perhaps **11** and **12** are best considered M(II) complexes with a ligand-localized radical (Scheme 3). This ligand radical is a one-electron oxidized imido ligand $(\cdot NAr)^-$ and exhibits properties of a rare imidyl radical that has only very recently been described in coordination chemistry.[25,26] The electronic configurations of **11** and **12** distinguish themselves from $[SiP^{iPr}_3]Fe(NAr)$,[5] whose DFT-predicted ground state (S = ½) is calculated to consist of a largely metal-centered radical.

In conclusion, we have introduced several well-defined examples of mononuclear Ru(I) and Os(I) complexes. These unusual complexes have been shown, through EPR simulations and DFT calculations, to consist of predominantly metal-centered radical character with a minority of the spin density delocalized onto the chelated phosphines. The reactivity of the dinitrogen adduct derivatives **3** and **4** were shown to exhibit formal M(I/III) group transfer reactivity. Detailed analysis of the imido/nitrene products suggests that they possess substantial imidyl radical character at the “ArN” moiety.

Acknowledgments

Supporting information for this article is available on the WWW under http://www.angewandte.org or from the author. CCDC-764569 – CCDC 764573 and CCDC-765970 – CCDC 765973 contain the supplementary crystallographic data for this paper. These data may be obtained free of charge from The Cambridge Crystallographic Data Centre via www.ccdc.com.ac.uk/data_request/cif.

References

1. de Bruin B, Hetterscheid DGH, Koekkoek AJJ, Grützmacher H. Prog. Inorg. Chem. 2007; 55:247.
2. a Bianchini C, Laschi F, Peruzzini M, Zanello P. Gazz. Chim. Ital. 1994; 124:271. Ru(I). b Angelici RJ, Zhu B, Fedi S, Laschi F, Zanello P. Inorg. Chem. 2007; 46:10901. [PubMed: 17999494] c Mulazzani QG, Emmi S, Fuochi PG, Hoffman MZ, Venturi M. J. Am. Chem. Soc. 1978; 100:981. d Robinson SD, Uttley MF. J. Chem. Soc., Dalton Trans. 1972:1. e Zotti G, Pilloni G, Bressan M, Martelli M. J. Electroanal. Chem. 1977; 75:607. Os(I). f Bianchini C, Peruzzini M, Ceccanti A, Laschi F, Zanello P. Inorg. Chim. Acta. 1997; 259:61. g Vugman NV, Rossi AM, Danon J. J. Chem. Phys. 1978; 68:3152. h Zotti G, Pilloni G, Bressan M, Martelli M. Inorg. Chim. Acta. 1978; 30:L311.
3. a Schröder, M.; Stephenson, TA. Comprehensive Coordination Chemistry. Wilkinson, G., editor. Vol. 4. Permagon Books Ltd.; Oxford: 1987. p. 277-519.b Griffith, WP. Comprehensive Coordination Chemistry. Wilkinson, G., editor. Vol. 4. Permagon Books Ltd.; Oxford: 1987. p. 519-635.c Housecroft, CE. Comprehensive Coordination Chemistry II. McCleverty, JA.; Meyer, TJ., editors. Vol. 5. Elsevier Ltd.; Oxford: 2004. p. 555-733.
4. a Mankad NP, Whited MT, Peters JC. Angew. Chem. Int. Ed. 2007; 46:5768. b Whited MT, Mankad NP, Lee Y, Oblad PF, Peters JC. Inorg. Chem. 2009; 48:2507. [PubMed: 19209938]
5. Mankad NP, Peters JC. J. Am. Chem. Soc. 2010 ASAP.
6. τ = (β- α)/60 where β and α represent the two largest angles. τ = 1 for TBP, 0 for square pyramid. See: Addison AW, Rao TN, Van Rijn JJ, Veschoor GC. J. Chem. Soc. Dalton Trans. 1984:1349.

7. A related series of N_2 complexes has been characterized for the corresponding iron system. See: Lee Y, Mankad NP, Peters JC. Nat. Chem. 2010 in press.
8. A crystal grown from a THF/pentane mixture at RT reveals a solid-state structure with neither N_2 or THF bound trans to the silyl anchor. This contrasts crystals grown from a CH_2Cl_2/pentane mixture at -35 °C that afforded the N_2 adduct structure **7**. Both the N_2-bound and N_2-free structures show an unusually close contact distance to one methyl group from the [SiP^{iPr}_3] ligand, indicative of an agostic interaction. See SI for structural details.
9. This sample was prepared from an independent route involving salt metathesis of complex **1** with $NaBAr^F_4$, ruling out any exchange process with impurities of **3** that would broaden the resonances of the spectrum.
10. a Lu CC, Bill E, Weyhermüller T, Bothe E, Wieghardt K. J. Am. Chem. Soc. 2008; 130:3181. [PubMed: 18284242] b Adhikari D, Mossin S, Basuli F, Huffman JC, Szilagyi RK, Meyer K, Mindiola DJ. J. Am. Chem. Soc. 2008; 130:3676. [PubMed: 18302384] c Harkins SB, Mankad NP, Miller AJ, Szilagyi RK, Peters JC. J. Am. Chem. Soc. 2008; 130:3478. [PubMed: 18298114] d Haneline MR, Heyduk AF. J. Am. Chem. Soc. 2006; 128:8410. [PubMed: 16802801]
11. de Bruin B, Hetterscheid D. Eur. J. Inorg. Chem. 2007:211.
12. Some complexes with large Δg have been found to be mainly ligand-based radicals. See: Miyazato Y, Wada T, Muckerman JT, Fujita E, Tanaka K. Angew. Chem. Int. Ed. 2007; 46:5728.
13. a Büttner T, Geier J, Frison G, Harmer J, Calle C, Schweiger A, Schönberg H, Grützmacher H. Science. 2005; 307:235. [PubMed: 15653498] b Cataldo L, Choua S, Berclaz T, Geoffroy M, Mézailles N, Avarvari N, Mathey F, Le Floch P. J. Phys. Chem. A. 2002; 106:3017.
14. Two mixed-valent dinuclear Ru complexes, each featuring a formal Ru(I) center, exhibit Δg values of 0.20 and 0.26. See: Sarkar B, Kaim W, Fiedler J, Duboc C. J. Am. Chem. Soc. 2004; 126:14706. [PubMed: 15535680]
15. Kober EM, Meyer TJ. Inorg. Chem. 1984; 23:3877.
16. Calculated from DFT optimized structures. See SI for details.
17. a Baird MC. Chem. Rev. 1988; 88:1217. b Paonessa RS, Thomas NC, Halpern J. J. Am. Chem. Soc. 1985; 107:4333.
18. a Brown SD, Betley TA, Peters JC. J. Am. Chem. Soc. 2003; 125:322. [PubMed: 12517130] b Nieto I, Ding F, Bontchev RP, Wang H, Smith JM. J. Am. Chem. Soc. 2008; 130:2716. [PubMed: 18266366] c Cowley RE, Eckert NA, Lehaïk J, Holland PL. Chem Commun. 2009:1760.
19. Selected examples: a Jayaprakash KN, Gunnoe TB, Boyle PD. Inorg. Chem. 2001; 40:6481. [PubMed: 11720504] b Liang JL, Huang JS, Zhou ZY, Cheung KK, Che CM. Chem. Eur. J. 2001; 7:2306.
20. Selected examples: a Burell AK, Steedman AJ. J. Chem. Soc., Chem. Commun. 1995:2109.; b Danopoulos AA, Wilkinson G, Hussain-Bates B, Hursthouse MB. Polyhedron. 1992; 11:2961.
21. Betley TA, Wu Q, Van Voorhis T, Nocera DG. Inorg. Chem. 2008; 47:1849. [PubMed: 18330975]
22. For a d^4 multiply bonded species in TBP geometry see; England J, Martinho M, Farquhar ER, Frisch JR, Bominaar EL, Münck E, Que L Jr. Angew. Chem. Int. Ed. 2009; 48:3622.
23. The calculated structure has *i*Pr groups replaced with Me groups and Ar = Ph instead of PhMe. τ = 0.49 for this compound. See ref. 5.
24. Ashford NA, Jarke FH, Solomon IJ. J. Chem. Phys. 1972; 57:3867.
25. Walstrom AN, Fullmer BC, Fan H, Pink M, Buschhorn DT, Caulton KG. Inorg. Chem. 2008; 47:9002. [PubMed: 18759426]
26. Lu CC, George SD, Weyhermüller T, Bill E, Bothe E, Wieghardt K. Angew. Chem. Int. Ed. 2008; 47:6384.

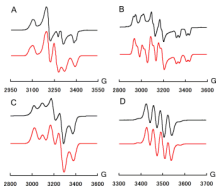

Figure 1.

A: 77 K EPR spectrum of **3**. (g_x, g_y, g_z) = (2.130, 2.076, 1.995). **B**: 77K EPR spectrum of **4**. (g_x, g_y, g_z) = (2.239, 2.133, 1.982) **C**: 77K EPR spectrum of **5**. (g_x, g_y, g_z) = (2.175, 2.075, 2.009). **D**: RT EPR spectrum of **11**. g_{iso} = 2.020. Red (bottom) curves represent simulations. See SI for other prarameters.

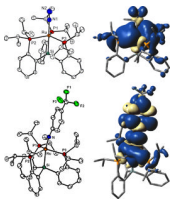

Figure 2.
Solid-state structures (50 % probability) and spin density plots (0.0004 isocontours) for **3** (top) and **11** (bottom). Selected bond lengths (Å) and angles (°): **3**, Ru-N1, 2.049(3); Ru-P1, 2.3221(9); Ru-P2, 2.3743(9); Ru-P3, 2.3253(9); Ru-Si, 3.2187(9); N1-N2, 1.097(5); Si-Ru-N1, 177.0(1); P1-Ru-P2, 109.53(3); P2-Ru-P3, 131.32(3); P1-Ru-P3, 111.85(3). **11**, Ru-N, 1.869(2); Ru-P1, 2.2968(7); Ru-P2, 2.4242(6); Ru-P3, 2.3756(7); Ru-Si, 2.3949(6); Si-Ru-N, 162.4(1), Ru-N-C(Ar), 172.0(2); P1-Ru-P2, 106.30(2); P2-Ru-P3, 130.24(2); P3-Ru-P1, 109.71(2).

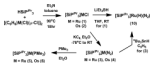

Scheme 1.

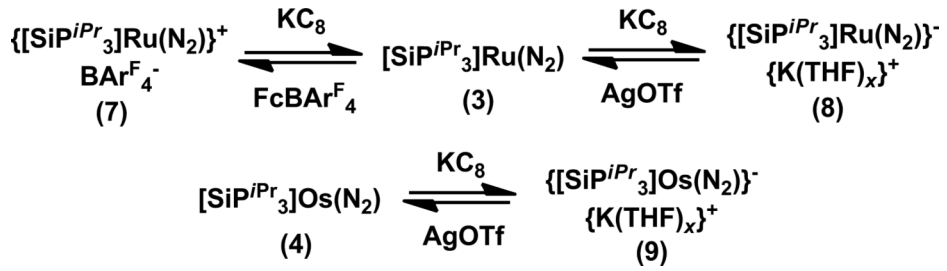

Scheme 2.

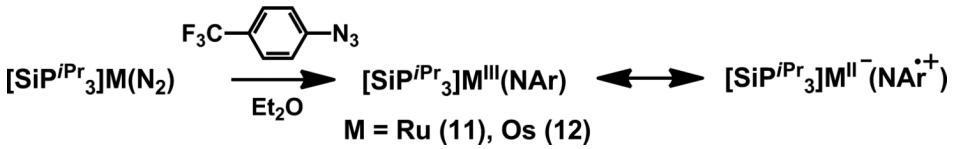

Scheme 3.